High-Pressure Raman and Luminescence Study on the Phase Transition of GdVO4:Eu3+ Microcrystals

ARTICLE *in* THE JOURNAL OF PHYSICAL CHEMISTRY C · OCTOBER 2010

Impact Factor: 4.77 · DOI: 10.1021/jp106063c

6 AUTHORS, INCLUDING:

Chuanchao Zhang
China Academy of Engineering Physics
11 PUBLICATIONS **44** CITATIONS
SEE PROFILE

Zengming Zhang
University of Science and Technology of C…
96 PUBLICATIONS **567** CITATIONS
SEE PROFILE

R. C. Dai
University of Science and Technology of C…
24 PUBLICATIONS **79** CITATIONS
SEE PROFILE

Wang Zhongping
University of Science and Technology of C…
33 PUBLICATIONS **111** CITATIONS
SEE PROFILE

High-Pressure Raman and Luminescence Study on the Phase Transition of $GdVO_4:Eu^{3+}$ Microcrystals

C. C. Zhang,[†] Z. M. Zhang,[‡] R. C. Dai,[†] Z. P. Wang,[‡] J. W. Zhang,[†] and Z. J. Ding*[,†]

Hefei National Laboratory for Physical Sciences at Microscale and Department of Physics and The Centre of Physical Experiments, University of Science and Technology of China, Hefei, Anhui 230026, P. R. China

Received: July 1, 2010; Revised Manuscript Received: August 29, 2010

The Raman and luminescence spectra of $GdVO_4:Eu^{3+}$ microcrystals have been measured in the pressure range from ambient pressure to 16.4 GPa at room temperature by using a diamond anvil cell. The discontinuities on Raman mode and luminescence intensity and the appearance of new Raman bands and luminescence peaks have provided strong evidence for a phase transition at 7.4 GPa from zircon-type to scheelite-type structure, and the zircon-type and scheelite-type phases coexist over a pressure range of 7.4−16.4 GPa. The scheelite-type phase is retained after release of pressure.

1. Introduction

Gadolinium vanadate ($GdVO_4$), like other rare earth vanadate compounds, crystallizes in the zircon-type structure (space group $I4_1/amd$) at ambient condition. Recently, $GdVO_4$ has attracted considerable attention because it is an excellent host material for phosphors and solid-state lasers because of its high energy-conversion efficiency, large thermal conductivity, and high thermal stability, and rare earth ions (Eu^{3+}, Nd^{3+}, Pr^{3+}, Ho^{3+}, Er^{3+}, Tm^{3+}, Yb^{3+}) doped $GdVO_4$ have been widely studied.[1−6]

Most of zircon-type ABO_4 compounds are known to undergo a pressure-induced phase transition from zircon-type to scheelite-type structure, such as silicates $ZrSiO_4$ and $HfSiO_4$,[7,8] tetragonal orthophosphates $YbPO_4$ and $LuPO_4$,[9] and rare earth arsenates.[10] Similar pressure-induced transition has been observed in rare earth vanadates. High-pressure Raman spectroscopic studies of YVO_4, $TbVO_4$, $DyVO_4$, and $LuVO_4$ with a diamond anvil cell (DAC) set have indicated an irreversible phase transition from zircon to scheelite structure.[11−13] The luminescence studies of $YVO_4:Eu^{3+}$ and $EuVO_4$ also show the zircon-to-scheelite-structure transition at high pressure. But the luminescence spectra of $YVO_4:Eu^{3+}$ and $EuVO_4$ with the scheelite structure show that Eu^{3+} ion is in a distorted D_{2d} symmetry instead of an S_4 symmetry site in the scheelite structure, which can be explained by considering only the first coordination sphere oxygen about the Eu^{3+} ion in an S_4 symmetry site in the scheelite structure.[14,15]

$GdVO_4$ is known to undergo a phase transition from temperature investigations in a Bridgman anvil apparatus. The high-pressure phase found from the quenched products in the ex situ static high-pressure experiments is a scheelite-type structure.[10] For a better understanding of the properties of $GdVO_4$, it is of interest to study the structural stability of $GdVO_4$ and the local environment of the doped rare earth ions from both fundamental and applied perspectives. In this paper, we present in situ Raman and luminescence studies of $GdVO_4:Eu^{3+}$ microcrystals under pressures ranging from ambient pressure to 16.4 GPa at room temperature.

* Corresponding author. E-mail: zjding@ustc.edu.cn.
[†] Hefei National Laboratory for Physical Sciences at Microscale and Department of Physics.
[‡] The Centre of Physical Experiments.

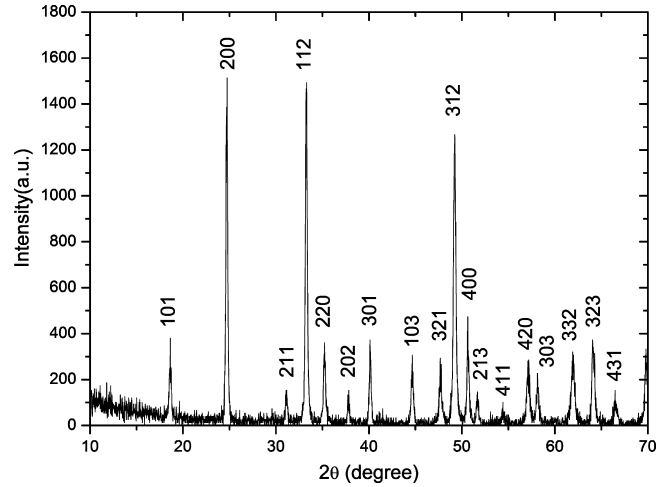

Figure 1. XRD pattern of $GdVO_4:Eu^{3+}$ microcrystals.

2. Experiment

The europium doped $GdVO_4$ sample (5 mol % Eu) was prepared by a hydrothermal method mostly according to the reported procedure.[1] The only difference is in the procedure of the hydrothermal conversion of the $Gd(OH)_3$ precursor. $Na_3VO_4 \cdot 12H_2O$ (1.6004 g) was first dissolved in 60 mL of distilled water, and then 20 mL of $Gd(OH)_3$ suspension was added with continuous stirring. The pH value of the mixture was adjusted by using 3 mL of 1 M NaOH solution. Then, the mixture was transferred into a 100 mL Teflon-lined autoclave. The autoclave was sealed and kept at 180 °C for 18 h. After that, fresh precipitates were separated by centrifugation, washed with deionized water and ethanol several times, followed by drying at 60 °C in air overnight. The crystal structure of the sample was studied by an X-ray diffraction apparatus (MAC Science MXP 18AHF) with Cu−Kα radiation. The X-ray diffraction pattern of the sample (Figure 1) identifies a pure phase of zircon-type structure (space group $I4_1/amd$), which is in good agreement with the JCPDS card 86-0996. The particle size of the sample was characterized by a field emission scanning electron microscope (SEM, Hitachi S-4800), and the SEM image in Figure 2 shows that the particle sizes are between 200 and 500 nm.

10.1021/jp106063c
Published on Web 10/07/2010

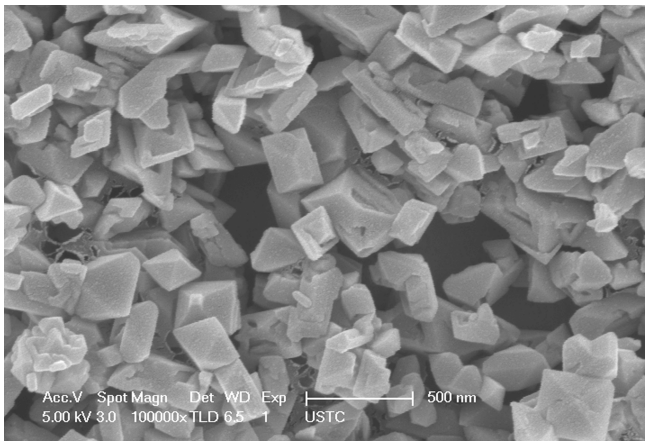

Figure 2. SEM image of $GdVO_4:Eu^{3+}$ microcrystals.

High-pressure measurements were carried out by a diamond anvil cell with 600 μm diameter culets. A stainless steel gasket was preindented, and then, a 170 μm hole was drilled by a spark eroder (BETSA, MH20M) to be used as the sample chamber. The methanol−ethanol (4:1 by volume) mixture was used as transmitting medium of hydrostatic pressure; the pressure was measured by the well-known ruby fluorescence technique.[16] By monitoring the separation and widths of both R_1 and R_2 lines, we confirmed that hydrostatic or quasi-hydrostatic condition was maintained throughout the experiment.

Raman and luminescence spectra were recorded by an integrated laser Raman system (LABRAM HR, Jobin Yvon) with a confocal microscope, a stigmatic spectrometer, and a multichannel air-cooled CCD detector with resolution of 1 cm^{-1}. The 488 nm line from an argon ion laser was used as the excitation source at a power level of 9.0 mW. All spectra were measured in the backscattering geometry at room temperature.

3. Results and Discussion

Pressure Effects on the Raman Spectra. $GdVO_4$ crystallizes in the zircon-type structure with space group $I4_1/amd$. The factor group analysis shows that there are 12 Raman active modes at the center of the Brillouin zone:[17]

$$\Gamma = 2A_{1g} + 4B_{1g} + B_{2g} + 5E_g$$

The measured Raman spectrum of the zircon-type $GdVO_4:Eu^{3+}$ microcrystals at ambient condition is shown at the bottom of Figure 3. Only 9 of 12 Raman active modes were observed in the Raman spectrum; they are in good agreement with the reported measurement.[17] The modes observed in the region 260−1000 cm^{-1} are internal stretching and bending vibrations of the VO_4 tetrahedra, and the modes observed at 124, 156, and 245 cm^{-1} are external ones. The Raman vibrational frequencies at ambient pressure with their mode assignments are given in Table 1.

The Raman spectra of $GdVO_4:Eu^{3+}$ microcrystals at several measured pressures and at room temperature are illustrated in Figure 3. With pressure increasing, all the Raman modes shift to higher frequencies except the external mode at 263 cm^{-1} that displays soft-mode behavior. At pressures up to 6.9 GPa, all Raman peaks can be assigned to the zircon-type phase. The pressure shifts of the Raman peak position below 6.9 GPa are computed by linear fits and are also listed in Table 1. At 7.4 GPa, an additional weak and broad peak first appears at 369 cm^{-1}. Another four new peaks with frequencies 146, 205, 326, and 458 cm^{-1} are observed when the pressure is increased to 8.1 GPa. In addition, three new peaks appear at 246, 783, and 827 cm^{-1} at 8.8 GPa, and at 9.6 GPa, another two new peaks appear at 198 and 437 cm^{-1}. With increasing pressure, the intensities of these new peaks become stronger, whereas the Raman peaks of the zircon-type $GdVO_4:Eu^{3+}$ gradually lose their intensities and become broad and indistinct. During the process of decompression down to ambient condition, the Raman spectra maintain a pattern similar to that of the high-pressure phase. Thus, the phase transition of $GdVO_4:Eu^{3+}$ is irreversible, and the recovered sample should have the same structure as that at high pressure. The pressure dependence of the frequencies for the observed Raman modes of $GdVO_4:Eu^{3+}$ are plotted in Figure 4. The discontinuities of the Raman modes with increasing pressure are clearly observed in the range of 7.4−9.6 GPa. Then, it can be concluded that a pressure-induced irreversible phase transition started at 7.4 GPa.

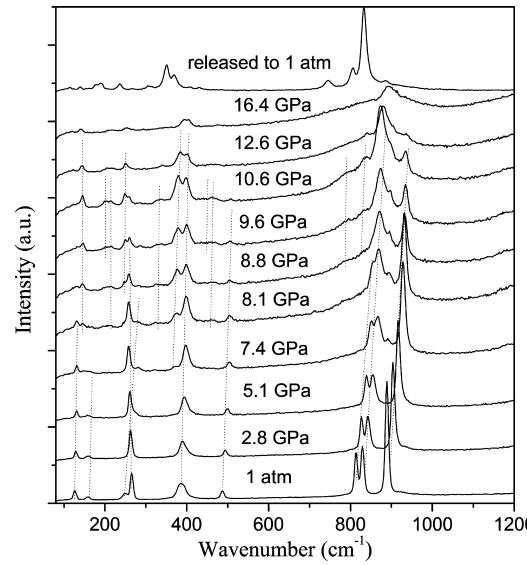

Figure 3. Raman spectra of $GdVO_4:Eu^{3+}$ at several pressures.

TABLE 1: Raman Frequencies ω_0, Mode Assignments, and their Pressure Derivatives of $GdVO_4:Eu^{3+}$ at Ambient Condition

zircon-type phase			scheelite-type phase		
mode type[a]	ω_0 (cm^{-1})	$d\omega/dP$ (cm^{-1}/GPa)	mode type[a]	ω_0 (cm^{-1})	$d\omega/dP$ (cm^{-1}/GPa)
T (B_{1g})	124	0.9	T (B_g)	140	−0.6
T or R (E_g)	156	0.1	T (E_g)	178	3.4
T or R (E_g)	245	4.5	T (E_g)	190	2.1
ν_2 (B_{2g})	263	−0.8	R (A_g)	236	1.0
ν_2 (A_{1g})	384	1.7	R (E_g)	307	2.8
ν_4 (B_{1g})	485	2.5	ν_2 (A_g)	350	2.3
ν_3 (B_{1g})	811	5.2	ν_2 (B_g)	370	1.0
ν_3 (E_g)	827	5.3	ν_4 (B_g)	407	2.6
ν_1 (A_{1g})	887	5.5	ν_4 (E_g)	432	1.7
			ν_3 (E_g)	745	2.8
			ν_3 (B_g)	804	1.6
			ν_1 (A_g)	833	3.2

[a] T = external translation, R = external rotation, ν = internal.

These changes in the Raman spectra are consistent with a pressure-induced zircon-to-scheelite phase transition observed in YVO_4,[11] $TbVO_4$, $DyVO_4$,[12] and $LuVO_4$.[13] The Raman spectrum of the high-pressure phase of $GdVO_4:Eu^{3+}$ is similar to those of the high-pressure phases of these rare earth vanadate compounds. Thus, it is concluded that an irreversible phase transition from the zircon-type to scheelite-type structure occurs

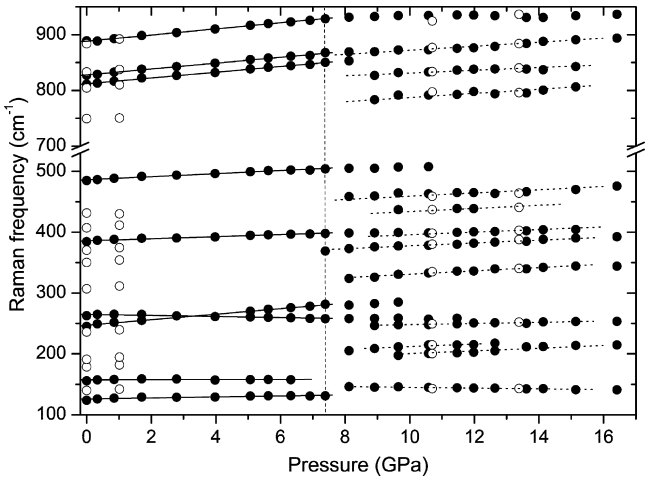

Figure 4. Pressure dependence of the shifts of Raman active modes. The solid and open symbols represent the data taken at increasing and decreasing pressure, respectively.

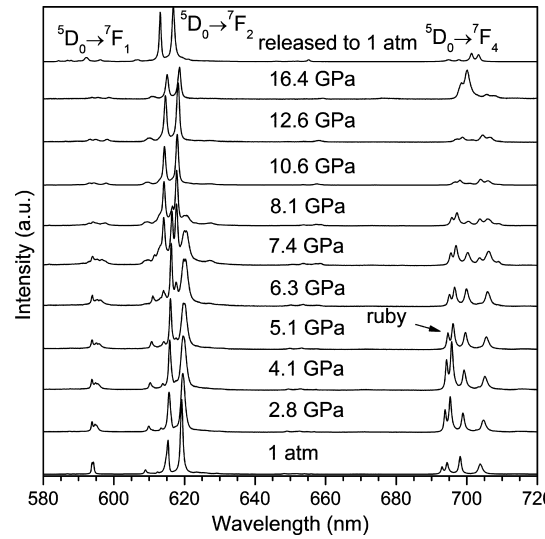

Figure 5. Luminescence spectra of $GdVO_4:Eu^{3+}$ at various pressures.

for $GdVO_4:Eu^{3+}$ at the pressure of 7.4 GPa at room temperature. For scheelite-type structure, group theory predicts 13 Raman active modes $3A_g + 5B_g + 5E_g$. Among these 13 Raman active modes, 12 modes are observed in Figure 3. The Raman modes and corresponding pressure shifts of scheelite-type $GdVO_4:Eu^{3+}$ are presented in Table 1. The mode assignments are made by comparing the Raman spectra with those of the high-pressure phases of YVO_4, $TbVO_4$, $DyVO_4$, and $LuVO_4$.[11−13]

It was found that the Raman modes of scheelite structure are predominant at pressures higher than 10.5 GPa and during the decompression down to ambient pressure. At pressure of 16.4 GPa, a weak peak corresponding to the symmetrical stretching mode of the zircon-type phase at 937 cm^{-1} was observed (Figure 3). After release to ambient pressure, two observed weak peaks at 265 and 885 cm^{-1} due to the symmetrical bending and the symmetrical stretching of zircon-type structure were also detected (Figure 3). The phenomena indicate that the phase transition of $GdVO_4:Eu^{3+}$ from zircon to scheelite structure was not entirely completed up to 16.4 GPa. Thus, its phase-transition behavior is different from that reported in YVO_4, $TbVO_4$, and $DyVO_4$ for which the phase transition under hydrostatic pressure is abrupt and rapid even at room temperature.[11,12] but it is similar to the pressure-induced phase-transition behavior of $LuVO_4$; two phases coexist within a wide pressure range.[13]

Stubican and Roy's[10] pressure−temperature equilibria curves for rare earth vanadates above 400 °C indicate that the transition pressure for $GdVO_4$ should be higher than those for $TbVO_4$ and $DyVO_4$ and lower than those for $LuVO_4$ and $EuVO_4$. The results agree with the observed zircon-to-scheelite phase-transition pressures in $GdVO_4:Eu^{3+}$ (7.4 GPa), $TbVO_4$ (6.6 GPa), $DyVO_4$ (6.5 GPa), and $LuVO_4$ (8 GPa) at room temperature.[12,13] But the transition pressure 7.4 GPa in $GdVO_4:Eu^{3+}$ is higher than 4.5 GPa for $EuVO_4$,[15] in disagreement with Stubican and Roy's equilibrium transition pressures for rare earth vanadates. The pressure−temperature equilibria curves for rare earth vanadates indicate that the transition pressure for $EuVO_4$ is higher than those for $GdVO_4$, $TbVO_4$, $DyVO_4$, and $LuVO_4$ above 400 °C. Chen et al. suggested that the lower transition pressure in $EuVO_4$ is due to a lower activation-energy barrier at room temperature for the zircon-type to scheelite-type structural phase transition in $EuVO_4$ relative to the same transition barriers in other rare earth vanadates.[15]

Pressure Effects on the Emission Spectra. In $GdVO_4$ lattice, the Eu^{3+} ions replace the Gd^{3+} ions with D_{2d} site symmetry. Group theory predicts four luminescence peaks from the $^5D_0 \rightarrow {}^7F_{1,2}$ transition in zircon-type $GdVO_4:Eu^{3+}$.[14,15] The luminescence spectrum of Eu^{3+} ions in $GdVO_4$ at ambient pressure is shown at the bottom of Figure 5. The sharp emission peaks due to $^5D_0 \rightarrow {}^7F_1$ transition are located at 593.7 and 594.2 nm, the two strongest lines from $^5D_0 \rightarrow {}^7F_2$ transition are at 615 and 619 nm, and the peaks at 698 and 704 nm are attributed to $^5D_0 \rightarrow {}^7F_4$ transition. The $^5D_0 \rightarrow {}^7F_3$ transition peaks are quite weak and indistinct under high pressure; therefore, only the peaks from transitions of $^5D_0 \rightarrow {}^7F_{1,2,4}$ were monitored with increasing pressure.

The evolution of the luminescence spectra obtained during the process of loading pressure at room temperature is shown in Figure 5. There are several obvious changes in the luminescence spectra during loading pressure. First, the two peaks for $^5D_0 \rightarrow {}^7F_1$ transition at ambient pressure are splitted into three ones at pressures higher than 2.8 GPa, indicating distortion of the local symmetry of Eu^{3+} ions and the complete removal of degeneracy of $^5D_0 \rightarrow {}^7F_1$ transition. Second, the two stronger peaks from $^5D_0 \rightarrow {}^7F_2$ transition gradually lose their intensity and become indistinct when pressure exceeds 8.1 GPa. During this process, the peak at 619 nm at ambient pressure is splitted into two peaks at pressures higher than 4.0 GPa and is too weak to be detected at 8.1 GPa. Meanwhile, the weakest peak at 612 nm at ambient pressure becomes more and more intensive with increasing pressure, and at 5.1 GPa, a new peak appears at 617 nm and becomes stronger with increasing pressure; these two peaks are prominent at pressures higher than 8.1 GPa. Third, two new peaks due to $^5D_0 \rightarrow {}^7F_4$ transition appear at 6.3 GPa. The drastic changes of the luminescence indicate the changes of the local symmetry of Eu^{3+} ions and the crystal field experienced by Eu^{3+} ions in the host material with increasing pressure.

Figure 6 shows the pressure-induced shifts of the luminescence peaks. The changes in the peak position are shown clearly at 7.4 GPa. Such behavior in luminescence spectra with increasing pressure suggests that the host materials may undergo a pressure-induced phase transition.

The $^5D_0 \rightarrow {}^7F_1$ transition is a magnetic-dipole allowed transition, and the intensity is supposed to be nearly independent from the crystal field. The $^5D_0 \rightarrow {}^7F_2$ transition is an enforced electric-dipole allowed transition, and the intensity depends strongly on the Eu^{3+} surrounding. It is widely accepted that the

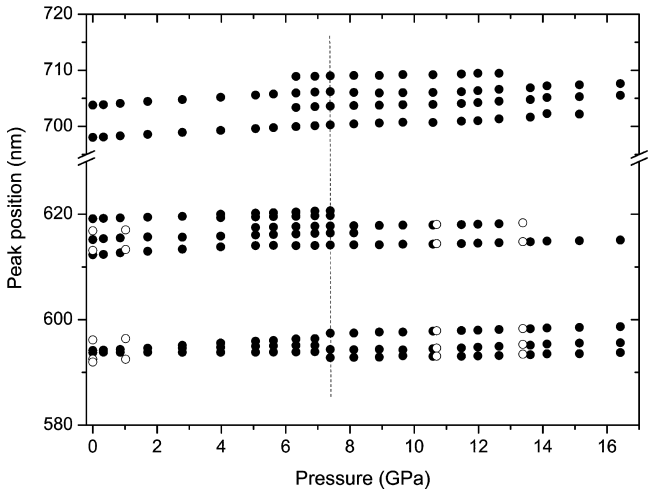

Figure 6. Pressure dependence of the luminescence peaks. The solid and open symbols represent the data taken at increasing and decreasing pressure, respectively.

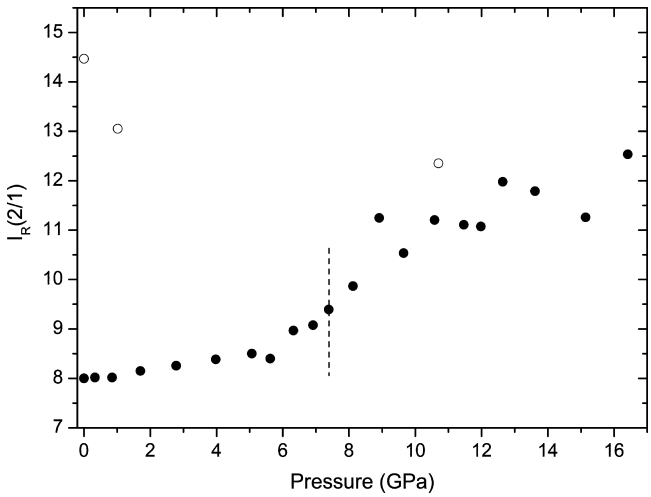

Figure 7. Pressure dependence of $I_R(2/1)$. The solid and open symbols represent the data taken at increasing and decreasing pressure, respectively.

luminescence intensity ratio of $^5D_0 \rightarrow {}^7F_1$ to $^5D_0 \rightarrow {}^7F_2$, $I_R(2/1)$, is an asymmetric factor. It depends on the covalency and/or local structure about Eu^{3+} ions. The higher the value of $I_R(2/1)$, the higher the asymmetry and covalence between Eu^{3+} and its surrounding will be.[18,19] The variation of $I_R(2/1)$ of $GdVO_4$:Eu^{3+} with pressure is shown in Figure 7, indicating that the asymmetry of Eu^{3+} ions increases obviously above transition pressure, and the symmetry of Eu^{3+} ions in the recovered sample is retained as that at high pressure. These characteristics of luminescence of $GdVO_4$:Eu^{3+} under pressure show that an irreversible phase transition occurs, which is consistent with the result observed by high-pressure Raman spectra.

4. Conclusion

The zircon-type $GdVO_4$:Eu^{3+} microcrystals with diameters of 200−500 nm were prepared by a hydrothermal method. The Raman and luminescence spectra of $GdVO_4$: Eu^{3+} microcrystals were measured in the pressure range from ambient pressure to 16.4 GPa at room temperature by a diamond anvil cell. The Raman-mode discontinuities and the appearance of new Raman peaks have provided strong evidence for a phase transition at a pressure of 7.4 GPa from zircon-type to scheelite-type structure, and the scheelite-type phase is retained after release of pressure. The changes on Eu^{3+} ion luminescence from $^5D_0 \rightarrow {}^7F_{1,2,4}$ transition in $GdVO_4$ were also observed at 7.4 GPa, which indicates that the site symmetry of Eu^{3+} ions in $GdVO_4$:Eu^{3+} microcrystals is changed under high pressure. The relative luminescence-intensity ratio of $^5D_0 \rightarrow {}^7F_1$ to $^5D_0 \rightarrow {}^7F_2$ transitions of Eu^{3+} ions is increasing obviously above transition pressure, indicating an increase of the asymmetry around Eu^{3+} ions with pressure. These observations show that the $GdVO_4$: Eu^{3+} microcrystals undergo a pressure-induced irreversible phase transition from zircon to scheelite structure at 7.4 GPa at room temperature.

Acknowledgment. This work was supported by the National Natural Science Foundation of China (Grant No. 10874160), National Basic Research Program of China (Grant No. 2009CB939901), Chinese Academy of Sciences, and Graduate Innovation Project of University of Science and Technology of China.

References and Notes

(1) Gu, M.; Liu, Q.; Mao, S. P.; Mao, D. L.; Chang, C. K. *Cryst. Growth Des.* **2008**, *8*, 1422–1425.
(2) Lisiecki, R.; Solarz, P.; Dominiak-Dzik, G.; Ryba-Romanowski, W.; Łukasiewicz, T. *Opt. Lett.* **2009**, *34*, 3271–3273.
(3) Chen, Y. F. *Opt. Lett.* **2004**, *29*, 2632–2634.
(4) Xu, W. W.; Xu, X. D.; Wang, J. Y.; Wu, F.; Su, L. B.; Zhao, G. J.; Zhao, Z. W.; Zhou, G. Q.; Xu, J. *J. Alloys Comp.* **2007**, *440*, 319–322.
(5) Singh, N. S.; Ningthoujam, R. S.; Yaiphaba, N.; Singh, S. D.; Vatsa, R. K. *Appl. Phys* **2009**, *105*, 064303.
(6) Lin, S. K.; Xiong, W.; Li, L. T.; Xie, Y. P. *J. Cryst. Growth* **2004**, *270*, 133–136.
(7) Knittle, E.; Williams, Q. *Am. Mineral.* **1993**, *78*, 245–252.
(8) Manoun, B.; Downs, R. T.; Saxena, S. K. *Am. Mineral.* **2006**, *91*, 1888–1892.
(9) Zhang, F. X.; Lang, M.; Ewing, R. C.; Lian, J.; Wang, Z. W.; Wu, J.; Boatner, L. A. *J. Solid State Chem.* **2008**, *181*, 2633–2638.
(10) Stubican, V. S.; Roy, R. *J. Appl. Phys.* **1963**, *34*, 1888–1890.
(11) Jayaraman, A.; Kourouklis, G. A.; Espinosa, G. P.; Cooper, A. S. *J. Phys. Chem. Solids* **1987**, *48*, 755–759.
(12) Duclos, S. J.; Jayaraman, A.; Espinosa, G. P.; Cooper, A. S. *J. Phys. Chem. Solids* **1989**, *50*, 769–775.
(13) Rao, R.; Garg, A. B.; Sakuntala, T.; Achary, S. N.; Tyagi, A. K. *J. Solid State Chem.* **2009**, *182*, 1879–1883.
(14) Chen, G.; Stump, N. A.; Haire, R. G.; Peterson, J. R.; Abraham, M. M. *J. Phys. Chem. Solids* **1992**, *53*, 1253–1257.
(15) Chen, G.; Haire, R. G.; Peterson, J. R.; Abraham, M. M. *J. Phys. Chem. Solids* **1994**, *55*, 313–316.
(16) Mao, H. K.; Bell, P. M.; Shaner, J. W.; Steinberg, D. J. *J. Appl. Phys.* **1978**, *49*, 3276–3283.
(17) Santos, C. C.; Silva, E. N.; Ayala, A. P.; Guedes, I.; Pizani, P. S.; Loong, C.-K.; Boatner, L. A. *J. Appl. Phys.* **2007**, *101*, 053511.
(18) Chen, G.; Haire, R. G.; Peterson, J. R. *J. Phys. Chem. Solids* **1995**, *56*, 1095–1100.
(19) Machon, D.; Dmitriev, V. P.; Sinitsyn, V. V.; Lucazeau, G. *Phys. Rev. B* **2004**, *70*, 094117.

JP106063C